

Diagnosis of Earth-Fill Dams by Several Sounding Tests

Shin-ichi NISHIMURA, Toshifumi SHIBATA and Takayuki SHUKU
Graduate School of Environmental and Life Science, Okayama Univ., Japan

Abstract. The spatial distribution of the strength inside an earth-fill dam is identified by sounding tests. In this research, the Swedish Weight Sounding (SWS) test is employed, and the spatially high-density test is possible to identify the spatial correlation structure by the SWS. The correlation structure of an earth-fill could be identified accurately based on the sounding results, and the high resolution of the spatial distribution could be visualized by using the indicator simulation. Consequently, it has been verified the practical use of the spatial distribution of the probability that the N-value is lower than the threshold value, may be used for the maintenance of an earth-fill dam.

Keywords. earth-fill dam, geostatistics, Swedish Weight Sounding, spatial variability

1. Introduction

There are many earth-fill dams in Japan. Some of them are getting old and decrepit, and therefore, have weakened. Making a diagnosis of the dams is important to increasing their lifetime, and an investigation of the strength inside the embankments is required for this task. In the present research, the spatial distribution of the strength parameters of dilapidated earth-fills is discussed, and an identification method for the distribution is proposed. Although the strength of the earth-fills is generally predicted from the standard penetration test (SPT) N-values, Swedish Wight Sounding (SWS) tests (e.g. JGS, 2004) are employed in this research as a static sounding method of obtaining the spatial distribution of the N-values. SWS tests are advantageous in that they make short interval examinations possible, because of their simplicity.

In general, the identification of the spatial correlation of soil parameters is difficult, since the usual sampling intervals are greater than the spatial correlation. Therefore, sounding tests are convenient for determining the correlation lengths. Tang (1979) determined the spatial correlation of a ground by cone penetration tests (CPT). Cafaro and Cherubini (1990) also evaluated the spatial correlation with the CPT results. Uzielli, et al. (2005) considered several

types of correlation functions for the CPT results. Nishimura and Shimizu (2008) determined the correlation parameters of N-value at a coastal dyke with the maximum likelihood method.

The information about the spatial correlation structures is important to perform the random field analyses. Fenton and Griffiths (2002), who analyzed the settlement of a footing on the ground, considering the spatial correlation structure of Young's modulus. In addition, Griffiths et al. (2002) calculated the bearing capacity by analyzing the random field of the undrained shear strength using the elasto-plastic finite element method. Bakker (2005) also analyzed the stability of a dyke using the elasto-plastic model based on the random field of the undrained shear strength. Nishimura et al. (2010) applied the random field theory to the elasto-plastic model and evaluated the risk of the earth-fill dams.

Firstly, the statistical models of the N-values are determined from the SWS tests results. For this task, the minimizing information criterion method is employed to evaluate the statistical model of an embankment, which involves the mean function and the covariance function. The semi-variograms also are estimated. Then, N-value distributions derived from sounding results are spatially interpolated with the indicator simulation (Deutsch and Journel 1992), which is

one of the geostatistical methods (Journal and Huijbregts, 1978).

2. Statistical Model of N-values

A representative variable for the soil properties, *s* is defined by Eq. (1) as a function of the location **X**=(*x*, *y*, *z*). Variable *s* is assumed to be expressed as the sum of the mean value *m* and the random variable *U*, which is a normal random variable in this study.

$$s(\mathbf{X}) = m(\mathbf{X}) + U(\mathbf{X}) \tag{1}$$

The random variable function, *s*(**X**), is discretized spatially into a random vector **s**^t=(*s*₁, *s*₂, ..., *s*_{*M*}), in which *s*_{*k*} is a point estimation value at the location **X**=(*x*_{*k*}, *y*_{*k*}, *z*_{*k*}). The soil parameters, which are obtained from the tests, are defined here as **S**^t=(*S*₁, *S*₂, ..., *S*_{*M*}). Symbol *M* signifies the number of test points. Vector **S** is considered as a realization of the random vector **s**^t=(*s*₁, *s*₂, ..., *s*_{*M*}). If the variables *s*₁, *s*₂, ..., *s*_{*M*} constitute the *M* - variate normal distribution, the probability density function of *s* can then be given by the following equation.

$$f_s(\mathbf{s}) = (2\pi)^{-M/2} |\mathbf{C}|^{-1/2} \times \exp\left\{-\frac{1}{2}(\mathbf{s} - \mathbf{m})^t \mathbf{C}^{-1}(\mathbf{s} - \mathbf{m})\right\} \tag{2}$$

in which **m**^t=(*m*₁, *m*₂, ..., *m*_{*M*}) is the mean vector of random function **s**^t=(*s*₁, *s*₂, ..., *s*_{*M*}); and it is assumed to be given by the regression function in Eq. (3). In this research, a 2-D statistical model is considered, namely, the horizontal coordinate *x*, which is parallel to the embankment axis, and the vertical coordinate *z* are introduced here, while the other horizontal coordinate *y*, which is perpendicular to the embankment axis, is disregarded.

$$\mathbf{m}_k = \mathbf{a}_0 + \mathbf{a}_1 \mathbf{x}_k + \mathbf{a}_2 \mathbf{z}_k + \mathbf{a}_3 \mathbf{x}_k^2 + \mathbf{a}_4 \mathbf{z}_k^2 + \mathbf{a}_5 \mathbf{x}_k \mathbf{z}_k \tag{3}$$

in which (*x*_{*k*}, *z*_{*k*}) are the coordinates of the position *k* where the function at that position, *s*_{*k*}

is given by Eq. (3) with the regression coefficients *a*₀, *a*₁, *a*₂, *a*₃, *a*₄, and *a*₅.

C is the *M*×*M* covariance matrix, which is selected from the following four covariance functions in this study.

$$\mathbf{C} = [C_{ij}] \begin{cases} \sigma^2 \exp\left(-|x_i - x_j|/l_x - |z_i - z_j|/l_z\right) & \text{(a)} \\ \sigma^2 \exp\left\{-\frac{(x_i - x_j)^2}{l_x^2} - \frac{(z_i - z_j)^2}{l_z^2}\right\} & \text{(b)} \\ \sigma^2 \exp\left\{-\sqrt{\frac{(x_i - x_j)^2}{l_x^2} + \frac{(z_i - z_j)^2}{l_z^2}}\right\} & \text{(c)} \\ N_e \sigma^2 \exp\left(-\frac{(x_i - x_j)}{l_x} - \frac{(z_i - z_j)}{l_z}\right) & \text{(d)} \end{cases} \tag{4}$$

i, j = 1, 2, \dots, M

$$\begin{cases} N_e = 1 & (i = j) \\ N_e \leq 1 & (i \neq j) \end{cases}$$

in which the symbol [*C*_{*ij*}] signifies an *i-j* component of the covariance matrix, σ is the standard deviation, and *l*_{*x*} and *l*_{*z*} are the correlation lengths for the *x* and *z* directions, respectively. Parameter *N*_{*e*} is related to the nugget effect. The Akaike's Information Criterion, AIC (Akaike 1974) is defined by Eq. (5), considering the logarithmic likelihood.

$$\begin{aligned} \text{AIC} &= -2 \cdot \max\{\ln f_s(\mathbf{S})\} + 2L \\ &= M \ln 2\pi \\ &\quad + \min\{\ln |\mathbf{C}| + (\mathbf{S} - \mathbf{m})^t \mathbf{C}^{-1}(\mathbf{S} - \mathbf{m})\} + 2L \end{aligned} \tag{5}$$

in which *L* is the number of unknown parameters included in Eq. (2). By minimizing AIC (MAIC), the regression coefficients of the mean function, the number of regression coefficients, the standard deviation, σ , the type of the covariance function, the nugget effect parameter, and the correlation lengths are determined.

Because the correlation lengths of soil parameters are often short compared with the sampling or the testing interval, sometimes the correlation lengths cannot be determined using the aforementioned method. For such cases, the following two-step approach is proposed as a strategy for identifying the spatial correlation structure. First, the mean (trend) function and the

variances are determined by MAIC. Subsequently, the covariance C_{ij} is determined from the semi-variogram. The semi-variogram is evaluated in the horizontal and vertical directions as individual functions of the sampling intervals.

$$\gamma_x(\mathbf{q} \cdot \Delta \mathbf{x}) = \frac{\sum_{j=1}^{N_x} \sum_{i=1}^{N_x - q} \{U(x_i, z_j) - U(x_i + q \cdot \Delta x, z_j)\}^2}{2N_x(N_x - q)}$$

$$\gamma_z(\mathbf{q} \cdot \Delta \mathbf{z}) = \frac{\sum_{j=1}^{N_z} \sum_{i=1}^{N_z - q} \{U(x_j, z_i) - U(x_j, z_i + q \cdot \Delta z)\}^2}{2N_z(N_z - q)} \quad (6)$$

$q = 1, 2, \dots$

where γ_x , and γ_z are the semi-variograms for the x , and the z axes, respectively, $U(x, z)$ is a measured parameter at the point (x, z) from which the mean value is removed, namely, the value of $(s(x, z) - m(x, z)) / \sigma$, Δx and Δz are sampling intervals, and N_x and N_z are the number of sampling points for the x and the z axes, respectively.

Next, the calculated semi-variograms are approximated by the following theoretical semi-variogram functions, and the correlation lengths are identified. Since an exponential type of function (Eq. (4a)) is selected as the best fitting function by MAIC in many cases, it is also employed here.

$$\gamma_x(|x_i - x_j|) = C_{0x} + C_{1x} \{1 - \exp(-|x_i - x_j| / l_x)\} \quad i \neq j$$

$$\gamma_z(|z_i - z_j|) = C_{0z} + C_{1z} \{1 - \exp(-|z_i - z_j| / l_z)\} \quad i \neq j$$

$$\gamma_x(0) = \gamma_z(0) = 0 \quad (7)$$

In Eq. (7), C_{0x} and C_{0z} are the parameters used for the nugget effect for the x and the z directions, respectively, and C_{1x} , and C_{1z} are the parameters used to express the shape of the semi-variogram functions.

Finally, the two-dimensional covariance C_{ij} between two points i and j , is given as

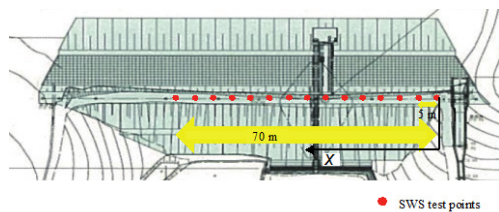


Figure 1. Plan view of embankment and testing interval.

$$C_{ij} = \sigma^2 C_{1x} C_{1z} \exp\left(-\frac{|x_i - x_j|}{l_x} - \frac{|z_i - z_j|}{l_z}\right) \quad i \neq j \quad (8)$$

$$C_{ij} = \sigma^2 \quad i = j$$

3. SWS Results and Geostatistical Analyses

3.1. In-situ Test Results

Although high-density sampling is required in order to evaluate the spatial distribution of soil parameters, the amount of data is not sufficient in the general sampling plans. In such cases, sounding is a convenient way to identify the spatial distribution structure of the soil parameters. In this research, an embankment at Site A is analyzed, for which SWS tests were conducted at fifteen points, at 5 m intervals, along the embankment axis, as shown in Figure 1. Additional tests were conducted between $x=18$ m and $x=24$ m with 2 m interval to identify the lateral correlation length. The soil profile for the embankment is categorized as intermediate soil, and consists of decomposed granite.

Generally, the strength parameters are assumed based on standard penetration tests (SPT) N-values with the use of empirical relationships. In this research, however, Swedish weight sounding (SWS) tests, which are simpler than SPT, are employed instead of SPTs. Inada (1960) derived the relationship in Eq. (9) between the results of SPT and SWS. Eq. (9) shows the relationship for sandy grounds, while Figure 2 shows the relationship between SWS and SPT N-values.

$$N_{SWS} = 0.002W_{SW} + 0.067N_{SW} \quad (9)$$

in which N_{SWS} is the N-value derived from SWS, N_{SW} is the number of half rations and W_{SW} is the total weight of the loads (N). Based on this data, the variability of the relationship is evaluated in this study, and the coefficient of variation is determined as 0.354. The determined σ -limits are also shown in Figure 2 with broken lines. Considering the variability of the relationship, the SPT N-value, N_{SPT} is modeled by

$$N_{SPT} = (1 + 0.354\varepsilon_r)N_{SWS} \tag{10}$$

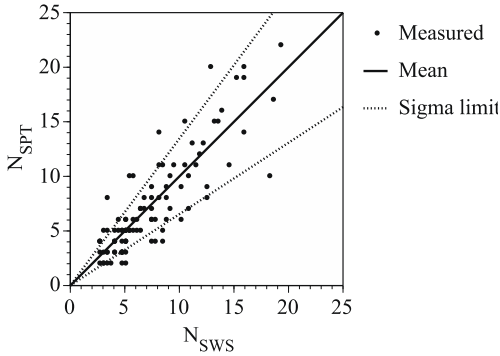


Figure 2. Relationship between SWS results and SPT N-values.

3.2. Statistical Model

The mean function and the covariance function of the SWS N-value, N_{SWS} , are determined with MAIC, and the mean is exhibited in Figure 3. The mean and the covariance functions given by Eqs. (3) and (4) were examined, and the optimum functions are determined as Eqs. (11) and (12). The horizontal correlation length l_x is identified as being approximately 10 m, and the vertical one l_z , is 2.66 m. Compared with the published values (Phoon and Kulhawy 1999, Tang 1979, DeGroot and Beacher 1993,

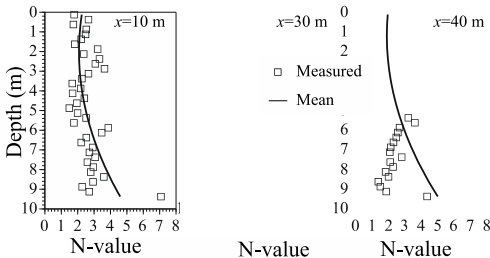
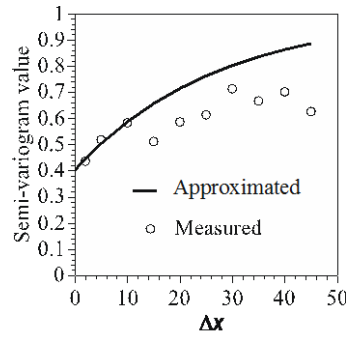
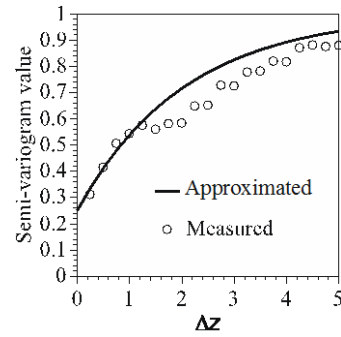


Figure 3. Distributions of SWS N-value.



(a) Horizontal



(b) Vertical

Figure 4. Semi-variograms and approximate functions.

Nishimura et al. 2010), the horizontal one is reasonable, and vertical one is rather large. The horizontal length, however, and almost three times the vertical one, and the values could be accepted by the fact that the horizontal length is much greater than the vertical one.

$$m = 2.52 - 0.0279x - 0.226z + 0.0003x^2 + 0.0465z^2 + 0.0038xz \tag{11}$$

$$[C_{ij}] = N_e \sigma^2 \exp(-\Delta x_i / l_x - \Delta z_j / l_z) \tag{12}$$

$$\begin{cases} N_e = 1 & (i = j) \\ N_e = 0.73 & (i \neq j) \end{cases}$$

$$\sigma = 1.08, l_x = 9.88\text{m}, l_z = 2.66\text{m}$$

To check the correlation structures, the semi-variograms for the horizontal and vertical directions are calculated. Figure 4 shows the semi-variograms. The semi-variogram values of $\Delta x = 2, 5, \text{ and } 10\text{m}$, $\Delta z = 0.25, 0.5, 0.75, 1.0, 1.25\text{ m}$ are employed to identify the approximate functions of Eq. (7) for the horizontal and vertical directions respectively, since the

accuracy of the semi-variogram values are high within the range of the small values of Δx and Δz . The optimum result is represented by the following function values.

$$C_{x1} \cdot C_{z1} = 0.45, l_x = 27.1m, l_z = 2.06m$$

The lateral correlation length is identified as being almost three times that of the MAIC, while the vertical length is determined as the value similar to that of the MAIC. There is the tendency generally that the variogram exhibits the relatively longer correlation distance, compared with the MAIC, since the correlation length is identified along the single coordinate in the case of the variogram.

3.3. Interpolated N-values

As for the mean and the covariance functions, Eqs. (11) and (12) are employed for the embankment. In the Monte Carlo simulation, random numbers for N_{SWS} are generated through the indicator simulation. Then, random numbers for N_{SPT} are created by considering the error factor ϵ_R in Eq. (10). The spatial statistical values for N_{SPT} are discussed below.

Figures 5 presents the analytical results. Figures 5 (a), (b), and (c) correspond to the mean, the standard deviation, and the probability that the N-values are smaller than 2.0, respectively.

According to Figures 5(a), around depth $z = 3-4$ m, $x = 30-40$ m, the lowest value is detected. Corresponding to Figure 5(a), the highest value of probability is obtained at the same location in Figure 5(c). The standard deviation value is positively correlated to the mean value, namely, the location of high mean N-value has high standard deviation as shown in Figure 5(b).

4. Conclusions

(1) With minimum lateral interval of SWS of 2 m, the spatial correlation structures of N-values inside the embankment could be evaluated accurately.

(2) Correlation structures were obtained by two approaches, MAIC and semi-variogram, and the difference of two results was acceptable.

(3) The spatial distribution of the probability that the N-value is lower than the threshold value (=2m, in this paper) has been calculated with the indicator simulation, and the weakened area could be identified visually. The spatially distribution of the probability can be used for the health monitoring of the inside of an embankment.

5. Acknowledgements

This work was partly supported by JSPS KAKENHI Grant Number 25292143

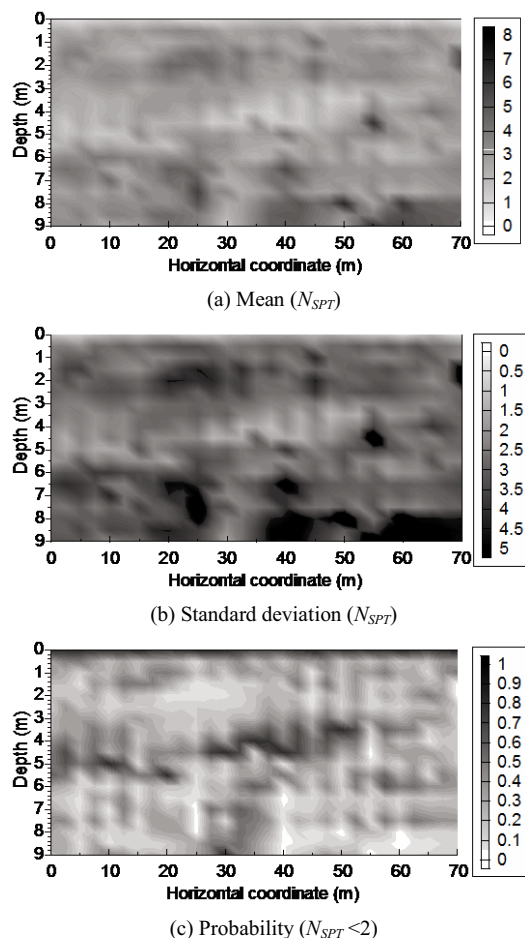


Figure 5. Statistical values of N_{SPT} by indicator simulation.

References

- Akaike, H. (1974). A new look at the statistical model identification, *IEEE Trans. on Automatic Control*, AC-19(6), 716-723.
- Bakker, H. L. (2005). Failure probability of river dykes strengthened with structural elements, *Proc. of 16th ICSMGE*, 1, 1845-1848.
- Cafaro, F. and Cherubini, C. (2002). Large sample spacing in evaluation of vertical strength variability of clayey soil, *Journal of Geotechnical and Geoenvironmental Engineering*, 128(7), 558-568.
- DeGroot, D. J. and Beacher, G. B. (1993). Estimating autocovariance of in-situ soft properties, *Journal of the geotechnical engineering*, ASCE, 119(1), 147-166.
- Deutsch, C. V. and Journel, A. G. (1992). *Geostatistical Software Library and User's Guide*, Oxford University Press.
- Fenton, G. A. and Griffiths, D. V. (2002). Probabilistic foundation settlement on spatial random soil, *Journal of Geotechnical and Geoenvironmental Engineering*, 128(5), 381-391.
- Griffiths, D. V., Fenton, G. A. and Manoharan N. (2002). Bearing capacity of rough rigid strip footing on cohesive soil: probabilistic study, *Journal of Geotechnical and Geoenvironmental Engineering*, 128(9), 743-755.
- Inada, M. (1960). Usage of Swedish weight sounding results, *Geotechnical Engineering Magazine*, 8(1), 13-18 (in Japanese).
- Japanese Geotechnical Society. (2004). *Japanese standards for geotechnical and geoenvironmental investigation methods – standards and explanations-*, Tokyo, JGS (in Japanese)
- Journel, A.G. and Huijbregts. (1978). *Mining geostatistics*, Academic Press.
- Nishimura, S., Murakami, A. and Matsuura, K. (2010). Reliability-based design of earth-fill dams based on the spatial distribution of strength parameters, *Georisk*, 4(3), 140-147.
- Nishimura, S. and Shimizu, H. (2008). Reliability-based design of ground improvement for liquefaction mitigation, *Structural Safety*, 30, 200-216.
- Phoon, K-K. and Kulhawy F.H. (1999). Evaluation of geotechnical property variability, *Can. Geotech. J.*, 36, 625-639.
- Soulie, P., Montes, P. and Silvestri, V. (1990). Modelling spatial variability of soil parameters, *Canadian Geotechnical Journal*, 27, 617-630.
- Tang, W. H. (1979). Probabilistic evaluation penetration resistances, *Journal of the geotechnical engineering*, ASCE, 105(GT10), 1173-1191.
- Uzielli, M., Vannucchi and Phoon, K. K. (2005). Random field characterization of stress-normalized cone penetration testing parameters, *Geotechnique*, 55(1), 3-20.